Connected Filters

Alexandre Xavier Falcão

Instituto de Computação - UNICAMP

afalcao@ic.unicamp.br

Introduction

- Mathematical morphology offers a variety of image transformations to eliminate dark (bright) regions from binary and grayscale images $\hat{I} = (D_I, I)$.

Introduction

- Mathematical morphology offers a variety of image transformations to eliminate dark (bright) regions from binary and grayscale images $\hat{I} = (D_I, I)$.
- The adjacency relation $\mathcal{A}$ plays the role of a planar structuring element. For example, the ball shape defined by

$$\mathcal{A}_r : \forall t \in \mathcal{N} = D_I, t \in \mathcal{A}_r(s) \quad \text{when} \quad \|t - s\|^2 \leq r^2, r \geq 1,$$

is very useful in several cases.

Introduction

- Two basic transformations are exact dilation $\Psi_D(\hat{I}, \mathcal{A}_r)$ and erosion $\Psi_E(\hat{I}, \mathcal{A}_r)$.

- Two basic transformations are exact dilation $\Psi_D(\hat{I}, \mathcal{A}_r)$ and erosion $\Psi_E(\hat{I}, \mathcal{A}_r)$.
- They create filtered images $\hat{V}_0 = (D_I, V_0)$, whose values $V_0(t)$ will constitute our initial connectivity map.

- Two basic transformations are exact dilation $\Psi_D(\hat{I}, \mathcal{A}_r)$ and erosion $\Psi_E(\hat{I}, \mathcal{A}_r)$.
- They create filtered images $\hat{V}_0 = (D_I, V_0)$, whose values $V_0(t)$ will constitute our initial connectivity map.
- Dilation and erosion are defined by

$$\begin{aligned} V_0(s) &= \max_{\forall t \in \mathcal{A}_r(s)} \{I(t)\} \\ V_0(s) &= \min_{\forall t \in \mathcal{A}_r(s)} \{I(t)\} \end{aligned}$$

respectively.

Introduction

Dilation and erosion can also be combined into other transformations, such as

Introduction

Dilation and erosion can also be combined into other transformations, such as

- Closing Ψ_C

$$\Psi_C(\hat{I}, \mathcal{A}_r) \quad = \quad \Psi_E(\Psi_D(\hat{I}, \mathcal{A}_r), \mathcal{A}_r)$$

Introduction

Dilation and erosion can also be combined into other transformations, such as

- Closing Ψ_C

$$\Psi_C(\hat{I}, \mathcal{A}_r) = \Psi_E(\Psi_D(\hat{I}, \mathcal{A}_r), \mathcal{A}_r)$$

- Opening Ψ_O

$$\Psi_O(\hat{I}, \mathcal{A}_r) = \Psi_D(\Psi_E(\hat{I}, \mathcal{A}_r), \mathcal{A}_r)$$

Dilation and erosion can also be combined into other transformations, such as

- Closing Ψ_C

$$\Psi_C(\hat{I}, \mathcal{A}_r) = \Psi_E(\Psi_D(\hat{I}, \mathcal{A}_r), \mathcal{A}_r)$$

- Opening Ψ_O

$$\Psi_O(\hat{I}, \mathcal{A}_r) = \Psi_D(\Psi_E(\hat{I}, \mathcal{A}_r), \mathcal{A}_r)$$

- Close-opening Ψ_{CO}

$$\Psi_{CO}(\hat{I}, \mathcal{A}_r) = \Psi_O(\Psi_C(\hat{I}, \mathcal{A}_r), \mathcal{A}_r)$$

Dilation and erosion can also be combined into other transformations, such as

- Closing Ψ_C

$$\Psi_C(\hat{I}, \mathcal{A}_r) = \Psi_E(\Psi_D(\hat{I}, \mathcal{A}_r), \mathcal{A}_r)$$

- Opening Ψ_O

$$\Psi_O(\hat{I}, \mathcal{A}_r) = \Psi_D(\Psi_E(\hat{I}, \mathcal{A}_r), \mathcal{A}_r)$$

- Close-opening Ψ_{CO}

$$\Psi_{CO}(\hat{I}, \mathcal{A}_r) = \Psi_O(\Psi_C(\hat{I}, \mathcal{A}_r), \mathcal{A}_r)$$

- Open-closing Ψ_{OC}

$$\Psi_{OC}(\hat{I}, \mathcal{A}_r) = \Psi_C(\Psi_O(\hat{I}, \mathcal{A}_r), \mathcal{A}_r)$$

However, they may create undesirable "side effects".

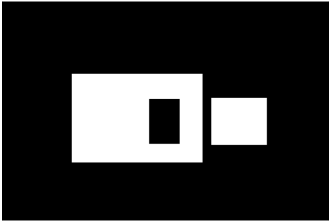

- Binary image with an undesired hole.

Introduction

However, they may create undesirable "side effects".

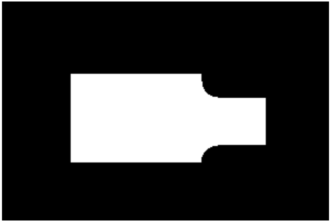

- Binary image with an undesired hole.
- Closing it by $\mathcal{A}_{15}$.

However, they may create undesirable "side effects".

- Binary image with an undesired hole.
- Closing it by $\mathcal{A}_{15}$.
- Close-opening it using $\mathcal{A}_{15}$.

Connected filters can correct those side effects by reconstructing the original shapes from $\hat{V}_0$ without bringing back the dark (bright) regions eliminated from $\hat{I}$ in the first operation.

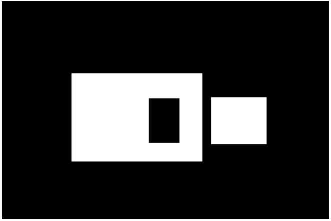

- Image $\hat{I}$ (mask).

Connected filters can correct those side effects by reconstructing the original shapes from $\hat{V}_0$ without bringing back the dark (bright) regions eliminated from $\hat{I}$ in the first operation.

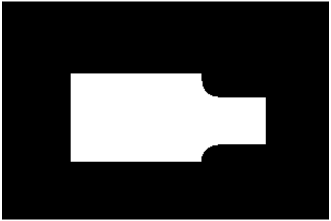

- Image $\hat{I}$ (mask).
- Image $\hat{V}_0 = \Psi_C(\hat{I}, \mathcal{A}_{15})$ (marker).

Connected filters can correct those side effects by reconstructing the original shapes from $\hat{V}_0$ without bringing back the dark (bright) regions eliminated from $\hat{I}$ in the first operation.

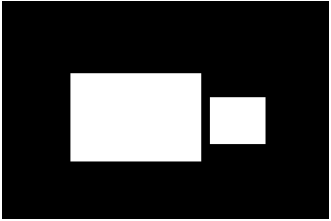

- Image $\hat{I}$ (mask).
- Image $\hat{V}_0 = \Psi_C(\hat{I}, \mathcal{A}_{15})$ (marker).
- Image $\hat{V}$ (our optimum connectivity map) after reconstruction of $\hat{I}$ from $\hat{V}_0$.

Organization of this lecture

- Basic definitions.

Organization of this lecture

- Basic definitions.
- Superior and inferior reconstructions [1, 2].

Organization of this lecture

- Basic definitions.
- Superior and inferior reconstructions [1, 2].
- Their relation with watershed-based segmentation [2, 3, 4].

Organization of this lecture

- Basic definitions.
- Superior and inferior reconstructions [1, 2].
- Their relation with watershed-based segmentation [2, 3, 4].
- Fast binary filtering [5].

Flat zones

- An image $\hat{I} = (D_I, I)$ may be interpreted as a discrete surface whose points have coordinates $(x_t, y_t, I(t)) \in \mathcal{Z}^3$.

Flat zones

- An image $\hat{I} = (D_I, I)$ may be interpreted as a discrete surface whose points have coordinates $(x_t, y_t, I(t)) \in \mathcal{Z}^3$.
- This surface contains

Flat zones

- An image $\hat{I} = (D_I, I)$ may be interpreted as a discrete surface whose points have coordinates $(x_t, y_t, I(t)) \in \mathcal{Z}^3$.
- This surface contains
  - domes — bright regions,

Flat zones

- An image $\hat{I} = (D_I, I)$ may be interpreted as a discrete surface whose points have coordinates $(x_t, y_t, I(t)) \in \mathcal{Z}^3$.
- This surface contains
  - domes — bright regions,
  - basins — dark regions, and

Flat zones

- An image $\hat{I} = (D_I, I)$ may be interpreted as a discrete surface whose points have coordinates $(x_t, y_t, I(t)) \in \mathcal{Z}^3$.
- This surface contains
  - domes — bright regions,
  - basins — dark regions, and
  - flat zones or plateaus — connected components with the same value and maximum area.

Connected filters essentially remove domes and/or basins, increasing the flat zones, such that any pair of spels in a given flat zone of the input image must belong to a same flat zone of the filtered image.

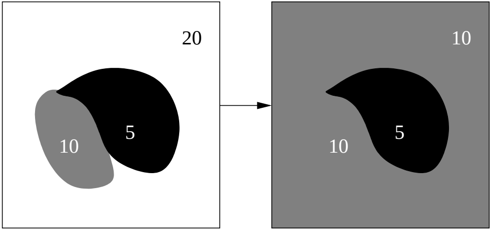

Regional minima and maxima

Regional minima (maxima) are flat zones whose values are strictly lower (higher) than the values of the adjacent spels. Considering a 4-neighborhood relation in the image below,

7	6	7	4	1	5	5
8	4	4	5	1	2	5
4	6	7	2	1	5	5
1	3	8	3	5	7	6
7	4	8	3	5	8	6
8	8	8	3	5	7	7

can you find minima and maxima?

Regional minima and maxima

Regional minima (maxima) are flat zones whose values are strictly lower (higher) than the values of the adjacent spels. Considering a 4-neighborhood relation in the image below,

7	6	7	4	1	5	5
8	4	4	5	1	2	5
4	6	7	2	1	5	5
1	3	8	3	5	7	6
7	4	8	3	5	8	6
8	8	8	3	5	7	7

MINIMA

Regional minima (maxima) are flat zones whose values are strictly lower (higher) than the values of the adjacent spels. Considering a 4-neighborhood relation in the image below,

7	6	7	4	1	5	5
8	4	4	5	1	2	5
4	6	7	2	1	5	5
1	3	8	3	5	7	6
7	4	8	3	5	8	6
8	8	8	3	5	7	7

MAXIMA

Superior reconstruction

- The superior reconstruction of $\hat{I}$ from $\hat{V}_0$ requires

$$V_0(t) \quad \geq \quad I(t)$$

for all $t \in D_I$.

Superior reconstruction

- The superior reconstruction of $\hat{I}$ from $\hat{V}_0$ requires

$$V_0(t) \quad \geq \quad I(t)$$

  for all $t \in D_I$.
- It repeats $\Psi_E(\hat{V}_0, \mathcal{A}_1) \cup \hat{I}$ multiple times up to the idempotence:

$$\Psi_E(\Psi_E(\hat{V}_0, \mathcal{A}_1) \cup \hat{I}, \mathcal{A}_1) \cup \hat{I} \ldots)$$

Instead of that, for every point t, the IFT finds a path from a regional minimum in $\hat{V}_0$ (component X) whose maximum altitude to reach t along that path is minimum.

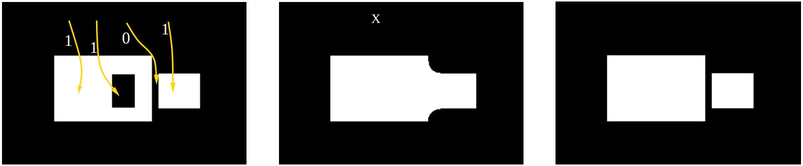

$\hat{I} = (D_I, I)$ $\hat{V}_0 = (D_I, V_0)$ $\hat{V} = (D_I, V)$

The IFT minimizes

$$V(t) = \min_{\forall \pi_t \in \Pi(D_I, \mathcal{A}_1, t)} \{ f_{srec}(\pi_t) \}$$

where f_{srec} is defined by

$$\begin{aligned} f_{srec}(\langle t \rangle) &= V_0(t) \\ f_{srec}(\pi_s \cdot \langle s, t \rangle) &= \max\{ f_{srec}(\pi_s), I(t) \}. \end{aligned}$$

Superior reconstruction by IFT

Indeed, the problem could also be easily solved without the closing operation, by marker imposition

$$V_0(t) = \begin{cases} I(t) & \text{if } t \in \mathcal{S}, \\ +\infty & \text{otherwise,} \end{cases}$$

where $\mathcal{S}$ represents seed spels (e.g., the border of $\hat{I}$).

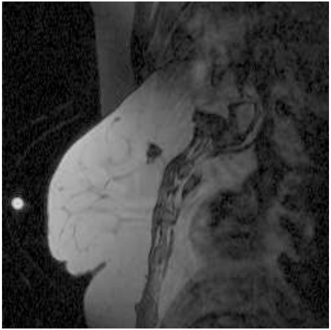

- Original image of a carcinoma.

Superior reconstruction by IFT

Indeed, the problem could also be easily solved without the closing operation, by marker imposition

$$V_0(t) = \begin{cases} I(t) & \text{if } t \in \mathcal{S}, \\ +\infty & \text{otherwise,} \end{cases}$$

where $\mathcal{S}$ represents seed spels (e.g., the border of $\hat{I}$).

- Original image of a carcinoma.
- Its binarization.

Superior reconstruction by IFT

Indeed, the problem could also be easily solved without the closing operation, by marker imposition

$$V_0(t) = \begin{cases} I(t) & \text{if } t \in \mathcal{S}, \\ +\infty & \text{otherwise,} \end{cases}$$

where $\mathcal{S}$ represents seed spels (e.g., the border of $\hat{I}$).

- Original image of a carcinoma.
- Its binarization.
- A closing of basins (marker imposition).

Indeed, the problem could also be easily solved without the closing operation, by marker imposition

$$V_0(t) = \begin{cases} I(t) & \text{if } t \in \mathcal{S}, \\ +\infty & \text{otherwise,} \end{cases}$$

where $\mathcal{S}$ represents seed spels (e.g., the border of $\hat{I}$).

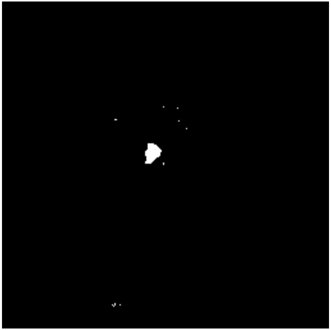

- Original image of a carcinoma.
- Its binarization.
- A closing of basins (marker imposition).
- Its residue.

Superior reconstruction by IFT

Indeed, the problem could also be easily solved without the closing operation, by marker imposition

$$V_0(t) = \begin{cases} I(t) & \text{if } t \in \mathcal{S}, \\ +\infty & \text{otherwise,} \end{cases}$$

where $\mathcal{S}$ represents seed spels (e.g., the border of $\hat{I}$).

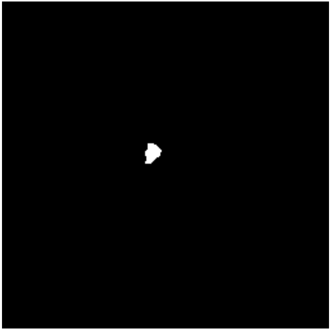

- Original image of a carcinoma.
- Its binarization.
- A closing of basins (marker imposition).
- Its residue.
- An opening by reconstruction.

Inferior reconstruction by IFT

- Similarly, the inferior reconstruction of $\hat{I}$ from $\hat{V}_0$ requires

$$V_0(t) \quad \leq \quad I(t)$$

for all $t \in D_I$ in order to eliminate domes rather than basins.

Inferior reconstruction by IFT

- Similarly, the inferior reconstruction of $\hat{I}$ from $\hat{V}_0$ requires

$$V_0(t) \quad \leq \quad I(t)$$

  for all $t \in D_I$ in order to eliminate domes rather than basins.
- In this case, for every point t, the IFT finds a path from a regional maxima in $\hat{V}_0$ whose minimum altitude to reach t along that path is maximum.

Inferior reconstruction by IFT

The IFT maximizes

$$V(t) \quad = \quad \max_{\forall \pi_t \in \Pi(D_I, \mathcal{A}_1, t)} \{f_{irec}(\pi_t)\}$$

for path function f_{irec} defined by

$$\begin{aligned} f_{irec}(\langle t \rangle) &= V_0(t) \\ f_{irec}(\pi_s \cdot \langle s, t \rangle) &= \min\{f_{irec}(\pi_s), I(t)\}. \end{aligned}$$

Inferior reconstruction by IFT

The IFT maximizes

$$V(t) = \max_{\forall \pi_t \in \Pi(D_I, \mathcal{A}_1, t)} \{f_{irec}(\pi_t)\}$$

for path function f_{irec} defined by

$$\begin{aligned} f_{irec}(\langle t \rangle) &= V_0(t) \\ f_{irec}(\pi_s \cdot \langle s, t \rangle) &= \min\{f_{irec}(\pi_s), I(t)\}. \end{aligned}$$

Marker imposition using a set $\mathcal{S}$ of seed spels is also valid.

$$V_0(t) = \begin{cases} I(t) & \text{if } t \in \mathcal{S}, \\ -\infty & \text{otherwise.} \end{cases}$$

Superior and inferior reconstructions

Therefore, we define

- the superior reconstruction by

$$\Psi_{srec}(\hat{I}, \hat{V}_0, \mathcal{A}_1), \hat{V}_0 \geq \hat{I},$$

Therefore, we define

- the superior reconstruction by

$$\Psi_{srec}(\hat{I}, \hat{V}_0, \mathcal{A}_1), \hat{V}_0 \geq \hat{I},$$

- the inferior reconstruction by

$$\Psi_{irec}(\hat{I}, \hat{V}_0, \mathcal{A}_1), \hat{V}_0 \leq \hat{I}.$$

Therefore, we define

- the superior reconstruction by

$$\Psi_{srec}(\hat{I}, \hat{V}_0, \mathcal{A}_1), \hat{V}_0 \geq \hat{I},$$

- the inferior reconstruction by

$$\Psi_{irec}(\hat{I}, \hat{V}_0, \mathcal{A}_1), \hat{V}_0 \leq \hat{I}.$$

- The way $\hat{V}_0$ is created gives other specific names to them.

For instance,

- Closing by reconstruction: $\hat{V}_0 = \Psi_C(\hat{I}, \mathcal{A}_r)$.

Superior and inferior reconstructions

For instance,

- Closing by reconstruction: $\hat{V}_0 = \Psi_C(\hat{I}, \mathcal{A}_r)$.
- Opening by reconstruction: $\hat{V}_0 = \Psi_O(\hat{I}, \mathcal{A}_r)$.

Superior and inferior reconstructions

For instance,

- Closing by reconstruction: $\hat{V}_0 = \Psi_C(\hat{I}, \mathcal{A}_r)$.
- Opening by reconstruction: $\hat{V}_0 = \Psi_O(\hat{I}, \mathcal{A}_r)$.
- h-Basins: residue $\Psi_{srec}(\hat{I}, \hat{V}_0) - \hat{I}$, $\hat{V}_0 = \hat{I} + h$, and $h \geq 1$.

For instance,

- Closing by reconstruction: $\hat{V}_0 = \Psi_C(\hat{I}, \mathcal{A}_r)$.
- Opening by reconstruction: $\hat{V}_0 = \Psi_O(\hat{I}, \mathcal{A}_r)$.
- h-Basins: residue $\Psi_{srec}(\hat{I}, \hat{V}_0) - \hat{I}$, $\hat{V}_0 = \hat{I} + h$, and $h \geq 1$.
- h-domes: residue $\hat{I} - \Psi_{irec}(\hat{I}, \hat{V}_0)$, $\hat{V}_0 = \hat{I} - h$, and $h \geq 1$.

Superior and inferior reconstructions

For instance,

- Closing by reconstruction: $\hat{V}_0 = \Psi_C(\hat{I}, \mathcal{A}_r)$.
- Opening by reconstruction: $\hat{V}_0 = \Psi_O(\hat{I}, \mathcal{A}_r)$.
- h-Basins: residue $\Psi_{srec}(\hat{I}, \hat{V}_0) - \hat{I}$, $\hat{V}_0 = \hat{I} + h$, and $h \geq 1$.
- h-domes: residue $\hat{I} - \Psi_{irec}(\hat{I}, \hat{V}_0)$, $\hat{V}_0 = \hat{I} - h$, and $h \geq 1$.
- Closing of basins or opening of domes: $\hat{V}_0$ is created by marker imposition.

Superior and inferior reconstructions can also be combined into a leveling transformation to correct edge blurring created by linear smoothing [6].

- Original image.

Superior and inferior reconstructions can also be combined into a leveling transformation to correct edge blurring created by linear smoothing [6].

- Original image.
- Regular Gaussian filtering.

Levelings

Superior and inferior reconstructions can also be combined into a leveling transformation to correct edge blurring created by linear smoothing [6].

- Original image.
- Regular Gaussian filtering.
- Leveling transformation.

This leveling operator uses the following sequence of transformations from $\hat{I}$ and the impaired image $\hat{V}_0$.

Algorithm

– LEVELING ALGORITHM

1. $\mathbf{X} \leftarrow \Psi_D(\hat{V}_0, \mathcal{A}_1) \cap \hat{I}$.
2. $\mathbf{I_R} \leftarrow \Psi_{iref}(\hat{I}, \mathbf{X}, \mathcal{A}_1)$.
3. $\mathbf{Y} \leftarrow \Psi_E(\hat{I}, \mathcal{A}_1) \cup \mathbf{I_R}$.
4. $\mathbf{S_R} \leftarrow \Psi_{srec}(\mathbf{I_R}, \mathbf{Y}, \mathcal{A}_1)$.

Superior reconstruction computation

For superior reconstruction:

- First, all nodes $t \in D_I$ are trivial paths with initial connectivity values $V_0(t)$.

Superior reconstruction computation

For superior reconstruction:

- First, all nodes $t \in D_I$ are trivial paths with initial connectivity values $V_0(t)$.
- The initial roots are identified at the global minima of $V_0(t)$.

Superior reconstruction computation

For superior reconstruction:

- First, all nodes $t \in D_I$ are trivial paths with initial connectivity values $V_0(t)$.
- The initial roots are identified at the global minima of $V_0(t)$.
- They may conquer their adjacent nodes by offering them better paths.

Superior reconstruction computation

For superior reconstruction:

- First, all nodes $t \in D_I$ are trivial paths with initial connectivity values $V_0(t)$.
- The initial roots are identified at the global minima of $V_0(t)$.
- They may conquer their adjacent nodes by offering them better paths.
- The process continues from the adjacent nodes in a non-decreasing order of path values.

$$\text{if } \max\{f_{srec}(\pi_s), I(t)\} < f_{srec}(\pi_t) \quad \text{then } \pi_t \leftarrow \pi_s \cdot \langle s, t \rangle.$$

Superior reconstruction computation

For superior reconstruction:

- First, all nodes $t \in D_I$ are trivial paths with initial connectivity values $V_0(t)$.
- The initial roots are identified at the global minima of $V_0(t)$.
- They may conquer their adjacent nodes by offering them better paths.
- The process continues from the adjacent nodes in a non-decreasing order of path values.

$$\text{if } \max\{f_{srec}(\pi_s), I(t)\} < f_{srec}(\pi_t) \quad \text{then } \pi_t \leftarrow \pi_s \cdot \langle s, t\rangle.$$

- Essentially the regional minima in $V_0(t)$ compete among themselves and some of them become roots (i.e., minima in $V(t)$).

The optimum-path forest with filtered values $V(t)$ (right) resulting from the superior reconstruction of $\hat{I} = (D_I, I)$ (left) from marker $\hat{V}_0 = (D_I, V_0)$ (center) contains unconquered regions (black dots) and the winner regional minima (red dots) as roots.

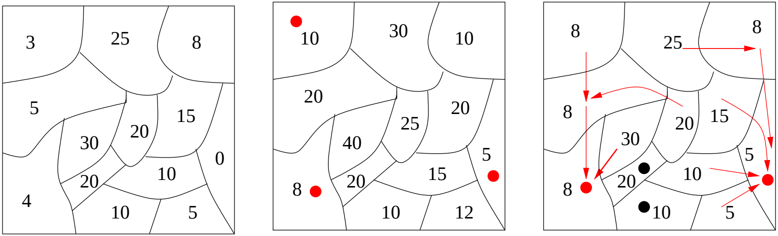

Images $\hat{I}$ (left), $\hat{V}_0$ (center), and $\hat{V}$ (right).

Algorithm

– SUPERIOR RECONSTRUCTION ALGORITHM

1. For each $t \in D_I$, do
2. Set $V(t) \leftarrow V_0(t)$.
3. If $V(t) \neq +\infty$, then insert t in Q.
4. While Q is not empty, do
5. Remove from Q a spel s such that $V(s)$ is minimum.
6. For each $t \in \mathcal{A}_1(s)$ such that $V(t) > V(s)$, do
7. Compute $tmp \leftarrow \max\{V(s), I(t)\}$.
8. If $tmp < V(t)$, then
9. If $V(t) \neq +\infty$, remove t from Q.
10. Set $V(t) \leftarrow tmp$.
11. Insert t in Q.

Organization of this lecture

- Basic definitions.
- Superior and inferior reconstructions.
- Their relation with watershed-based segmentation.
- Fast binary filtering.

Suppose we make a hole in each minimum of an image $\hat{I}$ and submerge its surface in a lake, such that each hole starts a flooding with water of different color. A watershed segmentation is obtained by preventing the mix of water from different colors.

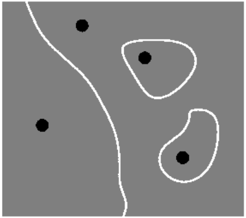

- Original image $\hat{I}$.

Superior reconstruction and watershed transform

Suppose we make a hole in each minimum of an image $\hat{I}$ and submerge its surface in a lake, such that each hole starts a flooding with water of different color. A watershed segmentation is obtained by preventing the mix of water from different colors.

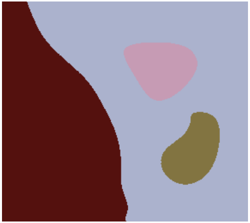

- Original image $\hat{I}$.
- IFT-watershed segmentation.

Superior reconstruction and watershed transform

Suppose we make a hole in each minimum of an image $\hat{I}$ and submerge its surface in a lake, such that each hole starts a flooding with water of different color. A watershed segmentation is obtained by preventing the mix of water from different colors.

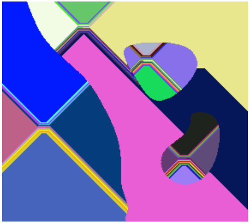

- Original image $\hat{I}$.
- IFT-watershed segmentation.
- Classical watershed segmentation requires to detect and label each minimum before the flooding process.

Superior reconstruction and watershed transform

- During superior reconstruction, we may force each regional minimum in $\hat{I}$ to produce a single optimum-path tree in P with a distinct label in L.

- During superior reconstruction, we may force each regional minimum in $\hat{I}$ to produce a single optimum-path tree in P with a distinct label in L.
- By definition, the resulting optimum-path forest is a watershed segmentation.

Superior reconstruction and watershed transform

- During superior reconstruction, we may force each regional minimum in $\hat{I}$ to produce a single optimum-path tree in P with a distinct label in L.
- By definition, the resulting optimum-path forest is a watershed segmentation.
- Moreover, by choice of $\hat{V}_0$, we may also eliminate the influence zones of "irrelevant" minima and considerably reduce the over-segmentation problem.

- During superior reconstruction, we may force each regional minimum in $\hat{I}$ to produce a single optimum-path tree in P with a distinct label in L.
- By definition, the resulting optimum-path forest is a watershed segmentation.
- Moreover, by choice of $\hat{V}_0$, we may also eliminate the influence zones of "irrelevant" minima and considerably reduce the over-segmentation problem.
- A change of topology in $\Psi_{srec}(\hat{I}, \hat{V}_0, \mathcal{A}_r)$ for $r > 1$ also helps on that.

Superior reconstruction and watershed transform

This requires a simple modification in f_{srec}.

$$f_{srec}(\langle t \rangle) = \begin{cases} I(t) & \text{if } t \in \mathcal{R}, \\ V_0(t) + 1 & \text{otherwise}, \end{cases}$$
$$f_{srec}(\pi_s \cdot \langle s, t \rangle) = \max\{f_{srec}(\pi_s), I(t)\},$$

where $\mathcal{R}$ is found on-the-fly with a single root for each regional minimum of the filtered image $\hat{V}$. The condition $V_0(t) + 1 > I(t)$ guarantees that all spels in D_I will be conquered.

Superior reconstruction and watershed transform

The choice of $V_0(t) = I(t) + h$, $h \geq 0$ will preserve all minima of $\hat{I}$ whose basins have depth greater than h. For $h = 0$, all minima will be preserved.

The choice of $V_0(t) = I(t) + h$, $h \geq 0$ will preserve all minima of $\hat{I}$ whose basins have depth greater than h. For $h = 0$, all minima will be preserved.

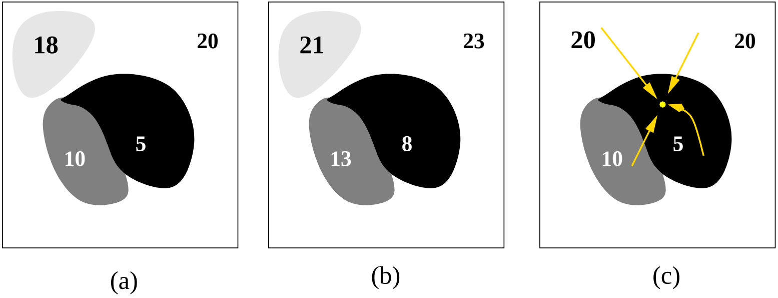

(a) Image $\hat{I}$. (b) Image $\hat{V}_0 + 1$ for $h = 2$. (c) Image $\hat{V} = \Psi_{srec}(\hat{I}, \hat{V}_0, \mathcal{A}_1)$ with indication of optimum paths in P.

Superior reconstruction and watershed transform

The choice of $V_0(t) = I(t) + h$, $h \geq 0$ will preserve all minima of $\hat{I}$ whose basins have depth greater than h. For $h = 0$, all minima will be preserved.

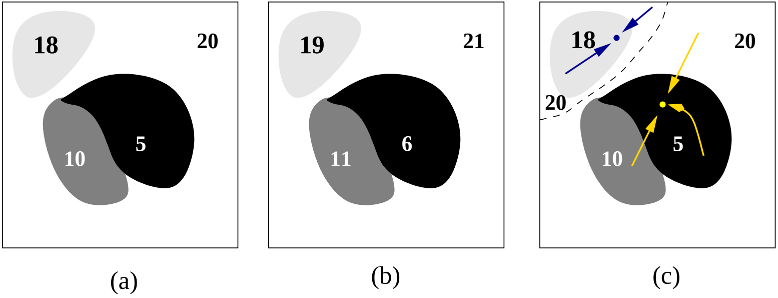

(a) Image $\hat{I}$. (b) Image $\hat{V}_0 + 1$ for $h = 0$. (c) Image $\hat{V} = \Psi_{srec}(\hat{I}, \hat{V}_0, \mathcal{A}_1)$ with indication of optimum paths in P.

Watershed from grayscale marker

For grayscale images $\hat{V}_0$, the simultaneous computation of a superior reconstruction in $\hat{V}$ and a watershed segmentation in L is called watershed from grayscale marker [4].

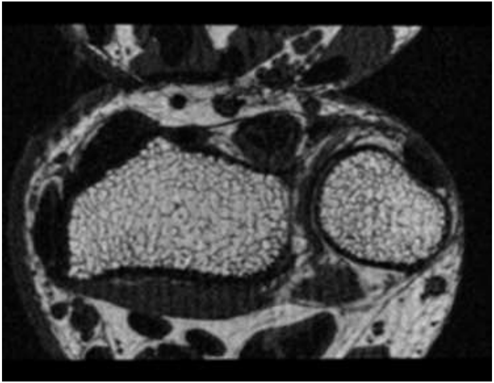

- MR-image of a wrist.

For grayscale images $\hat{V}_0$, the simultaneous computation of a superior reconstruction in $\hat{V}$ and a watershed segmentation in L is called watershed from grayscale marker [4].

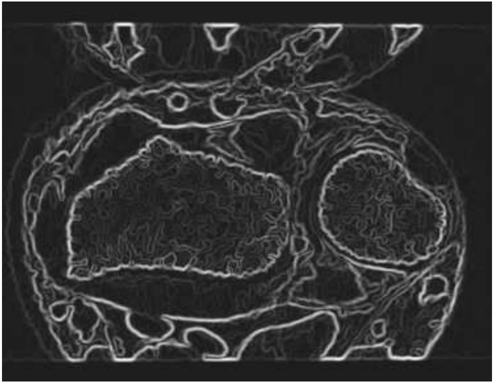

- MR-image of a wrist.
- A gradient image $\hat{I}$.

For grayscale images $\hat{V}_0$, the simultaneous computation of a superior reconstruction in $\hat{V}$ and a watershed segmentation in L is called watershed from grayscale marker [4].

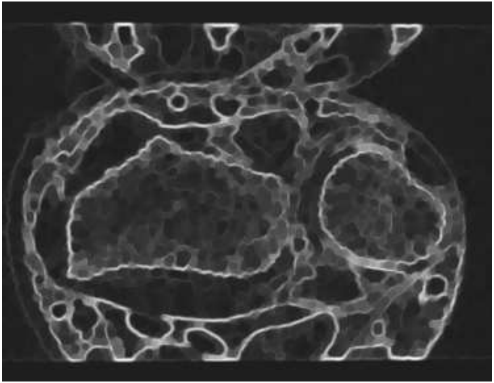

- MR-image of a wrist.
- A gradient image $\hat{I}$.
- The closing $\hat{V}_0 = \Psi_C(\hat{I}, \mathcal{A}_{2.5})$.

For grayscale images $\hat{V}_0$, the simultaneous computation of a superior reconstruction in $\hat{V}$ and a watershed segmentation in L is called watershed from grayscale marker [4].

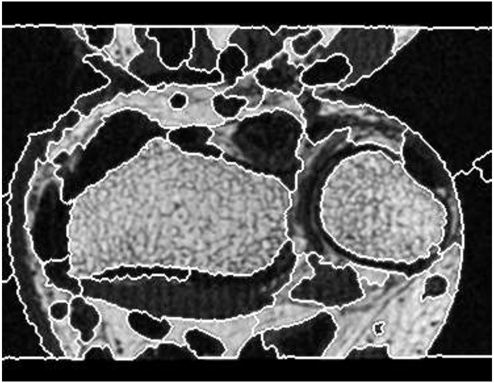

- MR-image of a wrist.
- A gradient image $\hat{I}$.
- The closing $\hat{V}_0 = \Psi_C(\hat{I}, \mathcal{A}_{2.5})$.
- Segmentation in L for $\Psi_{srec}(\hat{I}, \hat{V}_0, \mathcal{A}_{3.5})$.

Watershed from grayscale marker

Algorithm

– WATERSHED FROM GRAYSCALE MARKER

For each $t \in D_I$, *do*
  Set $P(t) \leftarrow nil$, $\lambda \leftarrow 1$, *and* $V(t) \leftarrow V_0(t) + 1$.
  Insert t *in* Q.
While Q *is not empty, do*
  Remove from Q *a spel* s *such that* $V(s)$ *is minimum*.
  If $P(s) = nil$ *then set* $V(s) \leftarrow I(s)$, $L(s) \leftarrow \lambda$, *and* $\lambda \leftarrow \lambda + 1$.
  For each $t \in \mathcal{A}(s)$ *such that* $V(t) > V(s)$, *do*
    Compute $tmp \leftarrow \max\{V(s), I(t)\}$.
    If $tmp < V(t)$, *then*
      Set $P(t) \leftarrow s$, $V(t) \leftarrow tmp$, $L(t) \leftarrow L(s)$.
      Update position of t *in* Q.

Organization of this lecture

- Basic definitions.
- Superior and inferior reconstructions.
- Their relation with watershed-based segmentation.
- Fast binary filtering.

For binary images $\hat{I}$ and Euclidean relations $\mathcal{A}_r$, it is also possible to exploit the IFT for fast computation of morphological operators, which can be decomposed into alternate sequences of erosions and dilations (or vice-versa). For instance,

$$
\begin{aligned}
\Psi_C(\hat{I}, \mathcal{A}_r) &= \Psi_E(\Psi_D(\hat{I}, \mathcal{A}_r), \mathcal{A}_r). \\
\Psi_{CO}(\hat{I}, \mathcal{A}_r) &= \Psi_D(\Psi_E(\Psi_E(\Psi_D(\hat{I}, \mathcal{A}_r), \mathcal{A}_r), \mathcal{A}_r), \mathcal{A}_r) \\
&= \Psi_D(\Psi_E(\Psi_D(\hat{I}, \mathcal{A}_r), \mathcal{A}_{2r}), \mathcal{A}_r). \\
\Psi_{CO}(\Psi_{CO}(\hat{I}, \mathcal{A}_r), \mathcal{A}_{2r}) &= \Psi_D(\Psi_E(\Psi_D(\Psi_E(\Psi_D(\hat{I}, \mathcal{A}_r), \mathcal{A}_{2r}), \\
&\quad \mathcal{A}_{3r}), \mathcal{A}_{4r}), \mathcal{A}_{2r}).
\end{aligned}
$$

Fast binary filtering via IFT

The basic idea is

- to extract the object's (background's) border $\mathcal{S}$,

Fast binary filtering via IFT

The basic idea is

- to extract the object's (background's) border $\mathcal{S}$,
- compute their propagation in sub-linear time outward (inward) the object for dilation (erosion), alternately.

Fast binary filtering via IFT

The basic idea is

- to extract the object's (background's) border $\mathcal{S}$,
- compute their propagation in sub-linear time outward (inward) the object for dilation (erosion), alternately.
- Each border propagation stops at the adjacency radius specified for dilation (erosion).

Fast binary filtering via IFT

This requires to constrain the computation of an Euclidean distance transform (EDT) either outside (dilation) or inside (erosion) the object up to a distance r from it.

The EDT assigns to every spel in D_I its distance to the closest spel in a given set $\mathcal{S} \subset D_I$ (e.g., the object's or background's border).

This requires to constrain the computation of an Euclidean distance transform (EDT) either outside (dilation) or inside (erosion) the object up to a distance r from it.

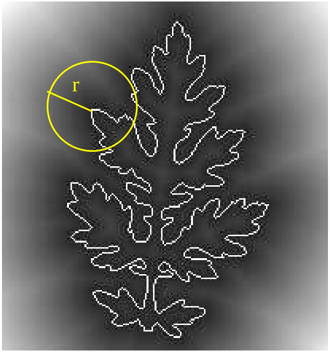

The EDT assigns to every spel in D_I its distance to the closest spel in a given set $\mathcal{S} \subset D_I$ (e.g., the object's or background's border).

Fast binary filtering via IFT

- A spel $s \in D_I$ belongs to an object's border $\mathcal{S}$, when $I(s) = 1$ and $\exists t \in \mathcal{A}_1(s)$, such that $I(t) = 0$. Similar definition applies to backgroud's border.

Fast binary filtering via IFT

- A spel $s \in D_I$ belongs to an object's border $\mathcal{S}$, when $I(s) = 1$ and $\exists t \in \mathcal{A}_1(s)$, such that $I(t) = 0$. Similar definition applies to backgroud's border.
- For dilation, the value 1 is propagated to every spel t with value $I(t) = 0$ and distance $\|t - R(\pi_t)\|^2 \leq r^2$, $R(\pi_t) \in \mathcal{S}$.

Fast binary filtering via IFT

- A spel $s \in D_I$ belongs to an object's border $\mathcal{S}$, when $I(s) = 1$ and $\exists t \in \mathcal{A}_1(s)$, such that $I(t) = 0$. Similar definition applies to backgroud's border.
- For dilation, the value 1 is propagated to every spel t with value $I(t) = 0$ and distance $\|t - R(\pi_t)\|^2 \leq r^2$, $R(\pi_t) \in \mathcal{S}$.
- For erosion, the value 0 is propagated to every spel t with value $I(t) = 1$ and distance $\|t - R(\pi_t)\|^2 \leq r^2$, $R(\pi_t) \in \mathcal{S}$.

Fast binary filtering via IFT

- A spel $s \in D_I$ belongs to an object's border $\mathcal{S}$, when $I(s) = 1$ and $\exists t \in \mathcal{A}_1(s)$, such that $I(t) = 0$. Similar definition applies to backgroud's border.
- For dilation, the value 1 is propagated to every spel t with value $I(t) = 0$ and distance $\|t - R(\pi_t)\|^2 \leq r^2$, $R(\pi_t) \in \mathcal{S}$.
- For erosion, the value 0 is propagated to every spel t with value $I(t) = 1$ and distance $\|t - R(\pi_t)\|^2 \leq r^2$, $R(\pi_t) \in \mathcal{S}$.
- During dilation (erosion), spels t whose distance $\|t - R(\pi_t)\|^2 > r^2$ but $\|P(t) - R(\pi_t)\|^2 \leq r^2$ are stored in a new set $\mathcal{S}'$ for a subsequent erosion (dilation) operation.

Fast binary filtering via IFT

The EDT is propagated in V from a set $\mathcal{S} \subset D_I$ to every spel $t \in D_I$ in a non-decreasing order of squared distance using $\mathcal{A}_{\sqrt{2}}$ in 2D (8-neighbors) [7]. For fast dilation, it uses path function

$$
\begin{aligned}
f_{euc}(\langle t \rangle) &= \begin{cases} 0 & \text{if } t \in \mathcal{S}, \\ +\infty & \text{if } I(t) = 0, \\ -\infty & \text{otherwise.} \end{cases} \\
f_{euc}(\pi_s \cdot \langle s, t \rangle) &= \|t - R(\pi_s)\|^2.
\end{aligned}
$$

Fast binary filtering via IFT

For fast erosion, it uses path function

$$
\begin{aligned}
f_{euc}(\langle t \rangle) &= \begin{cases} 0 & \text{if } t \in \mathcal{S}, \\ +\infty & \text{if } I(t) = 1, \\ -\infty & \text{otherwise.} \end{cases} \\
f_{euc}(\pi_s \cdot \langle s, t \rangle) &= \| t - R(\pi_s) \|^2.
\end{aligned}
$$

A dilated (eroded) binary image $\mathbf{J} = (D_I, J)$ is created during the distance propagation process.

Fast dilation

Algorithm

– FAST DILATION IN 2D UP TO DISTANCE r FROM $\mathcal{S}$

1. *For each* $t \in D_I$, *set* $J(t) \leftarrow I(t)$, $R(\pi_t) \leftarrow t$ *and* $V(t) \leftarrow f_{euc}(\langle t \rangle)$.
2. *While* $\mathcal{S} \neq \emptyset$, *remove* t *from* $\mathcal{S}$ *and insert* t *in* Q.
3. *While* Q *is not empty, do*
4.   *Remove from* Q *a spel* s *such that* $V(s)$ *is minimum.*
5.   *if* $V(s) \leq r^2$, *then*
6.   *Set* $J(t) \leftarrow 1$.
7.   *For each* $t \in \mathcal{A}_{\sqrt{2}}(s)$ *such that* $V(t) > V(s)$, *do*
8.   *Compute* $tmp \leftarrow \|t - R(\pi_s)\|^2$.
9.   *If* $tmp < V(t)$, *then*
10.   *If* $V(t) \neq +\infty$, *remove* t *from* Q.
11.   *Set* $V(t) \leftarrow tmp$ *and* $R(\pi_t) \leftarrow R(\pi_s)$.
12.   *Insert* t *in* Q.
13.   **Else** *insert* s *in* $\mathcal{S}$.

Sets $\mathcal{S}$ and $\mathcal{S}'$ may contain spels from multiple borders.

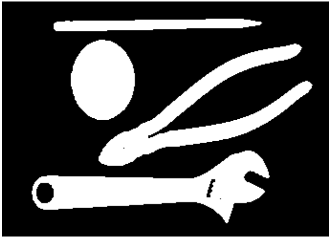

- Multiple borders,

Sets $\mathcal{S}$ and $\mathcal{S}'$ may contain spels from multiple borders.

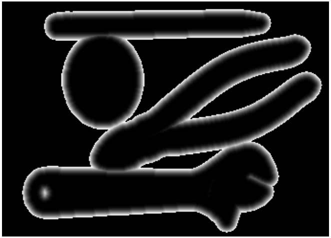

- Multiple borders,
- distances outside up to $r = 10$,

Sets $\mathcal{S}$ and $\mathcal{S}'$ may contain spels from multiple borders.

- Multiple borders,
- distances outside up to $r = 10$,
- their dilation,

Sets $\mathcal{S}$ and $\mathcal{S}'$ may contain spels from multiple borders.

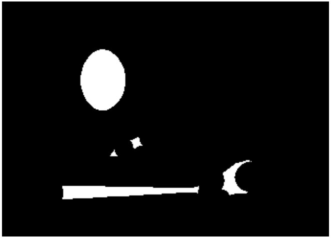

- Multiple borders,
- distances outside up to $r = 10$,
- their dilation,
- erosion,

Fast binary filtering via IFT

Sets $\mathcal{S}$ and $\mathcal{S}'$ may contain spels from multiple borders.

- Multiple borders,
- distances outside up to $r = 10$,
- their dilation,
- erosion,
- closing,

Sets $\mathcal{S}$ and $\mathcal{S}'$ may contain spels from multiple borders.

- Multiple borders,
- distances outside up to $r = 10$,
- their dilation,
- erosion,
- closing,
- closing by reconstruction,

Sets $\mathcal{S}$ and $\mathcal{S}'$ may contain spels from multiple borders.

- Multiple borders,
- distances outside up to $r = 10$,
- their dilation,
- erosion,
- closing,
- closing by reconstruction,
- opening, and

Sets $\mathcal{S}$ and $\mathcal{S}'$ may contain spels from multiple borders.

- Multiple borders,
- distances outside up to $r = 10$,
- their dilation,
- erosion,
- closing,
- closing by reconstruction,
- opening, and
- opening by reconstruction.

Fast 3D closing with $r = 20$ has been succesfully used in the visual inspection of focal cortical dysplastic (FCD) lesions — one of the major causes of refractory epilepsy [8].

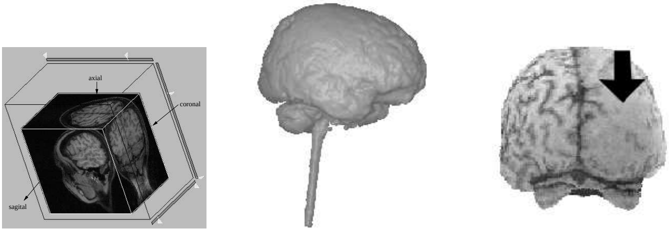

(a) (b) (c)

(a) 3D image $\hat{I}$. (b) Brain after closing. (c) FCD lesion.

3D visualization of cortical dysplastic lesions

After closing with $r = 20$, the texture of the 3D brain surface is presented in curvilinear cuts.

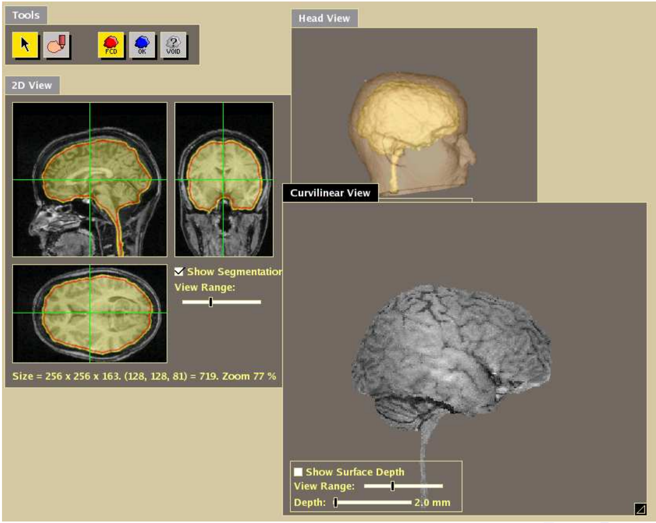

After closing with $r = 20$, the texture of the 3D brain surface is presented in curvilinear cuts.

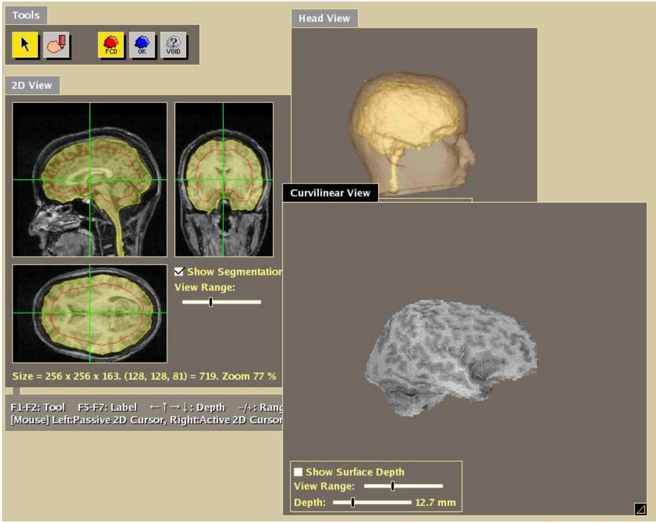

3D visualization of cortical dysplastic lesions

After closing with $r = 20$, the texture of the 3D brain surface is presented in curvilinear cuts.

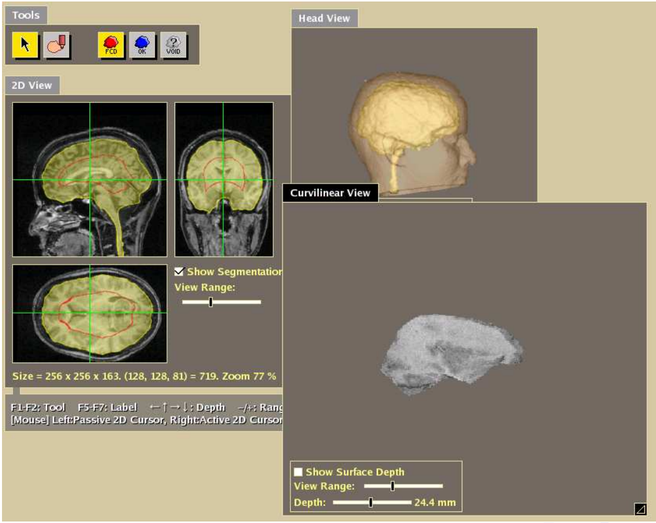

3D visualization of cortical dysplastic lesions

After closing with $r = 20$, the texture of the 3D brain surface is presented in curvilinear cuts.

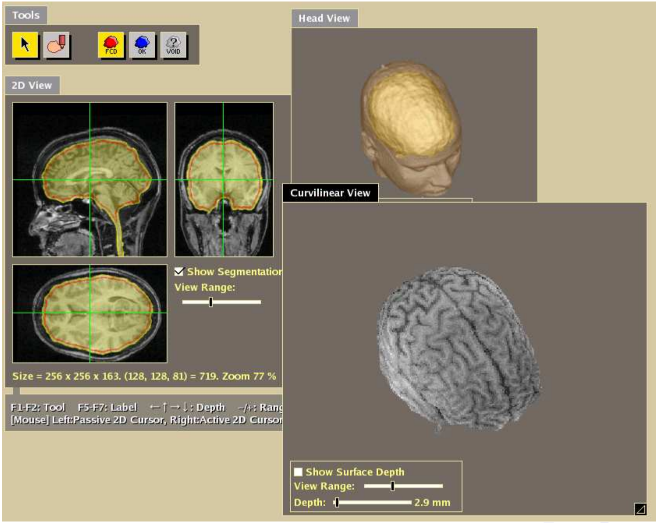

3D visualization of cortical dysplastic lesions

After closing with $r = 20$, the texture of the 3D brain surface is presented in curvilinear cuts.

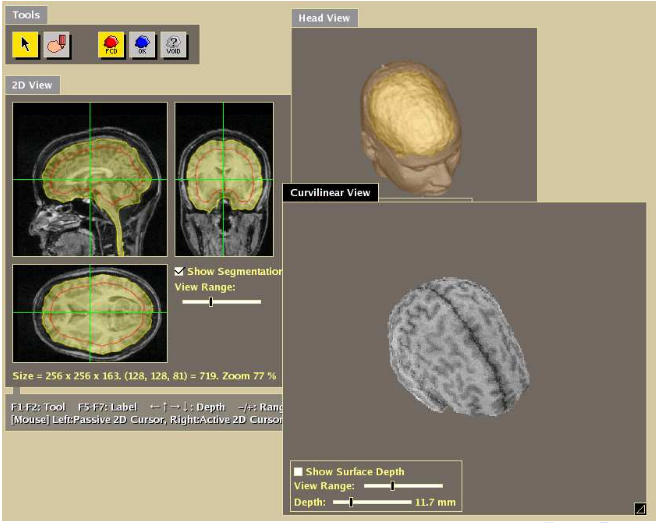

After closing with $r = 20$, the texture of the 3D brain surface is presented in curvilinear cuts.

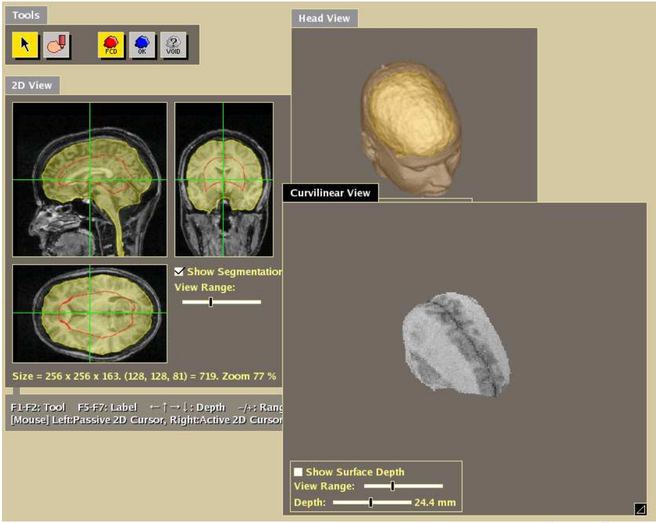

Conclusion

- The IFT framework has been demonstrated to the design of connected filters and for understanding the relation between watershed transform and superior reconstruction.

Conclusion

- The IFT framework has been demonstrated to the design of connected filters and for understanding the relation between watershed transform and superior reconstruction.
- It should be clear the advantages of a unified framework to understand the relation between different image operations.

Conclusion

- The IFT framework has been demonstrated to the design of connected filters and for understanding the relation between watershed transform and superior reconstruction.
- It should be clear the advantages of a unified framework to understand the relation between different image operations.
- We have also demonstrated the decomposition of some binary operators into alternate sequences of fast dilation and erosion by Euclidean IFT.

Conclusion

- The IFT framework has been demonstrated to the design of connected filters and for understanding the relation between watershed transform and superior reconstruction.
- It should be clear the advantages of a unified framework to understand the relation between different image operations.
- We have also demonstrated the decomposition of some binary operators into alternate sequences of fast dilation and erosion by Euclidean IFT.
- Finally, we have illustrated one application for these fast binary operators in 3D medical imaging.

[1] A.X. Falcão, J. Stolfi, and R.A. Lotufo.
The image foresting transform: Theory, algorithms, and applications.
IEEE Trans. on Pattern Analysis and Machine Intelligence, 26(1):19–29, 2004.

[2] A.X. Falcão, B. S. da Cunha, and R. A. Lotufo.
Design of connected operators using the image foresting transform.
In *SPIE on Medical Imaging*, volume 4322, pages 468–479, Feb 2001.

[3] R.A. Lotufo and A.X. Falcão.
The ordered queue and the optimality of the watershed approaches.
In *Mathematical Morphology and its Applications to Image and Signal Processing (ISMM)*, volume 18, pages 341–350. Kluwer, Jun 2000.

[4] R.A. Lotufo, A.X. Falcão, and F. Zampirolli.
IFT-Watershed from gray-scale marker.
In *XV Brazilian Symp. on Computer Graphics and Image Processing (SIBGRAPI)*, pages 146–152. IEEE, Oct 2002.

[5] I. Ragnemalm.

Fast erosion and dilation by contour processing and thresholding of distance maps.

Pattern Recognition Letters, 13:161–166, Mar 1992.

[6] Fernand Meyer.

Levelings, image simplification filters for segmentation.

Journal of Mathematical Imaging and Vision, 20(1-2):59–72, 2004.

[7] A.X. Falcão, L.F. Costa, and B.S. da Cunha.

Multiscale skeletons by image foresting transform and its applications to neuromorphometry.

Pattern Recognition, 35(7):1571–1582, Apr 2002.

[8] F. P. G. Bergo and A. X. Falcão.

Fast and automatic curvilinear reformatting of MR images of the brain for diagnosis of dysplastic lesions.

In *Proc. of 3rd Intl. Symp. on Biomedical Imaging*, pages 486–489. IEEE, Apr 2006.